Nonlinear optical properties of type-II quantum wells

G. R. Olbright, W. S. Fu,* and J. F. Klem
Sandia National Laboratories, Albuquerque, New Mexico 87185

H. M. Gibbs, G. Khitrova, R. Pon, B. Fluegel, K. Meissner, N. Peyghambarian,
R. Binder, I. Galbraith,† and S. W. Koch‡
Optical Sciences Center, University of Arizona, Tucson, Arizona 85721
(Received 28 February 1991)

Experimental and theoretical investigations of the near-band-gap optical nonlinearities in type-II GaAs/AlAs quantum wells are reported. The temporal evolution of the optical nonlinearities of different samples grown at our two different laboratories is analyzed by comparing femtosecond results at different pump-probe time delays with nanosecond measurements at different sample temperatures. The quasi-cw measurements at low temperatures show exciton bleaching and a pronounced heavy-hole exciton blueshift, which is absent at elevated plasma temperatures ($\simeq 100$ K). Femtosecond spectra show a delayed onset of the exciton blueshift consistent with hole-plasma cooling in the absence of electrons. The results are analyzed using many-body theory assuming complete electron-hole charge separation. We show that the presence of a one-component plasma modifies the nonlinear optical behavior of the GaAs layer and results in dramatically different properties compared to type-I quantum-well structures.

I. INTRODUCTION

In the past few years much attention has been focused on type-II GaAs/AlAs superlattices consisting of thin GaAs and AlAs layers, where the lowest-energy conduction-band state is confined to the indirect AlAs layer.[1–13] Ihm[1] showed that type-II superlattices are formed when the GaAs-layer thickness is less than $\simeq 35$ Å. For this case, the electron and hole plasmas become separated in both real and reciprocal spaces, resulting in a space-charge potential. The subsequent radiative recombination is indirect and correspondingly slow, on the order of microseconds.[5,6] Long lifetimes result in high-density electron and hole plasmas achievable with relatively low excitation intensities. Photoluminescence (PL) studies[2–6] provide direct evidence for electrons confined to the AlAs layer. Low-temperature PL spectra of indirect superlattices reveal two peaks, a high-energy peak corresponding to an electron-hole recombination at the GaAs Γ point, and a low-energy peak attributed to interlayer recombination of AlAs X-like electrons with GaAs Γ point holes. Danan *et al.*[7] investigated the behavior of the transition energies as a function of longitudinal electric field and reported a decrease in the Γ-X splitting with increased field. Menaydier *et al.*[8] observed evidence of an indirect-to-direct crossover through application of a longitudinal electric field. Subpicosecond transfer of electrons from the GaAs Γ point to the AlAs X point has been found.[9–11] Previously a blueshift of the indirect PL peak has been reported and explained in terms of the domination of the space-charge potential over other many-body effects.[6] Additionally an absorption blueshift of the heavy-hole exciton in type-II superlattices was observed.[12,13]

In this paper we present the complete temporal evolution of the optical nonlinearities in the absorption spectra of highly optically excited type-II GaAs/AlAs quantum wells using quasi-cw and femtosecond absorption spectroscopy. These investigations are performed on several type-II quantum-well structures having different Γ-X splitting which have been grown in our two different laboratories. The nonlinearities result in a strong bleaching of the inhomogeneously broadened heavy-hole (hh) exciton resonance. The bleaching is accompanied by a pronounced blueshift which develops on a 100-ps time scale.

This paper is organized as follows. We first present the linear optical properties of type-II heterostructures in Sec. II. In Sec. III we describe the effects of space-charge layers on the transition energies. In Sec. IV we present nanosecond nonlinear absorption spectra taken for different type-II samples. These samples were grown in different laboratories to allow conclusions which are independent of sample-specific properties. We show the excitation-dependent absorption for different Γ-X splitting and at different plasma temperatures. In Sec. V we present femtosecond time-resolved absorption spectra, both pumping into the band and into the exciton resonance, and discuss the complete temporal evolution of the optical nonlinearities. In Sec. VI we give a brief theoretical analysis of the nonlinear optical properties of type-II quantum wells, the technical details of which are reported in Ref. 14. Theory and experimental results are summarized and discussed in Sec. VII.

II. LINEAR OPTICAL PROPERTIES

In Fig. 1(a) we show the potential energy diagram of a typical GaAs/AlAs type-II heterostructure in real space.

The lowest direct transition (arrow labeled Γ-Γ in Fig. 1) has the energy

$$E_{\Gamma\text{-}\Gamma}=E_g^{\Gamma}+H_1+E_1-E_R^{\Gamma\text{-}\Gamma}\ , \tag{1}$$

where E_g^{Γ} is the bulk GaAs direct band gap, H_1 and E_1 are the confinement energies for the heavy hole and electron, respectively, and $E_R^{\Gamma\text{-}\Gamma}$ is the corresponding direct exciton binding energy. The energy of the lowest indirect transition (arrow labeled Γ-X in Fig. 1) is given as

$$E_{\Gamma\text{-}X}=E_g^{X}+H_1+E_1^{X}-E_R^{\Gamma\text{-}x}\ , \tag{2}$$

where E_g^X is the effective indirect band gap [i.e., the bulk AlAs indirect gap minus the offset of the Γ-valence bands at the GaAs/AlAs interface, which is $(1-0.67)\Delta E_g$ is the difference in the Γ-Γ band gaps of AlAs and GaAs], E_1^X is the confinement energy for electrons at the AlAs X valley, and $E_R^{\Gamma\text{-}X}$ is the binding energy of the indirect excitons. The difference between E_g^{Γ} and E_g^X is less than 200 meV. This difference can be easily surmounted by confinement energies of the GaAs electrons, which are very light ($m^*\simeq 0.067$). Thus for very narrow GaAs layers (<35 Å) the lowest-energy radiative transition is indirect as depicted in Fig. 1. The confinement energy of the AlAs X electrons is not as sensitive to thickness changes because of the larger effective masses.[1–5]

Whereas in the corresponding bulk material (AlAs) the X point exhibits a threefold degeneracy because of the equivalence of the momentum in the three spatial directions ([100], [010], and [001]). This degeneracy is lifted in quantum wells to a twofold degeneracy of the $X_{x,y}$ valley, describing the motion within the plane ([100] and [010]), and the X_z valley for electrons moving in growth direction [001]. This is a consequence of the fact that the lattice constant of AlAs is larger than that of the GaAs substrate, resulting in AlAs layers under biaxial compression. The lattice mismatch strain results in a lowering of the X_x and X_y valleys with respect to the X_z valley. Thus, for wide wells (little or no confinement of X-point electrons) the $X_{x,y}$ valley has the lowest energy for AlAs layers. However, for AlAs layers that are less than $\simeq 55$ Å wide the quantum confinement of the $X_{x,y}$ valley pushes its energy above the X_z valley because the mass of the $X_{x,y}$ valley is small ($m_{X_{x,y}}=0.19m_0$) compared to the mass of the X_z valley ($m_{X_z}=1.1m_0$).[15] We have sketched the lowest in-plane energy bands in Fig. 1(b), indicating the direct absorption, interlayer electron, and indirect recombination transitions, $\Gamma\rightarrow\Gamma$, $\Gamma\rightarrow X$, and $X\rightarrow\Gamma$, respectively.

Low-temperature PL spectra of type-II multiple quantum wells reveal two peaks: a high-energy peak corresponding to electron-hole recombination at the Γ point in GaAs (Fig. 2, solid PL peak labeled Γ-Γ) and a low-

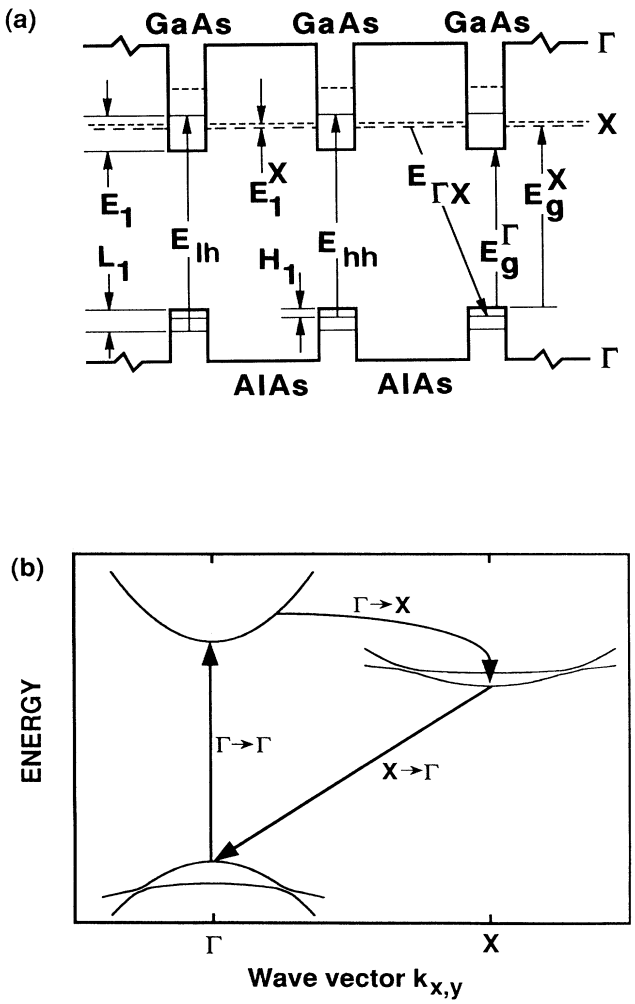

FIG. 1. Type-II quantum-well structure. (a) Quantum-well energy diagram in real space; E_g^{Γ} and E_g^X are the direct GaAs band gap and the effective indirect bandgap energies (see text); E_1, E_1^X, H_1, and L_1^{Γ} are the Γ-electron, X-electron, heavy-hole, and light-hole quantum-confinement energies, respectively. (b) Sketch of the in-plane band structure in the [100] direction.

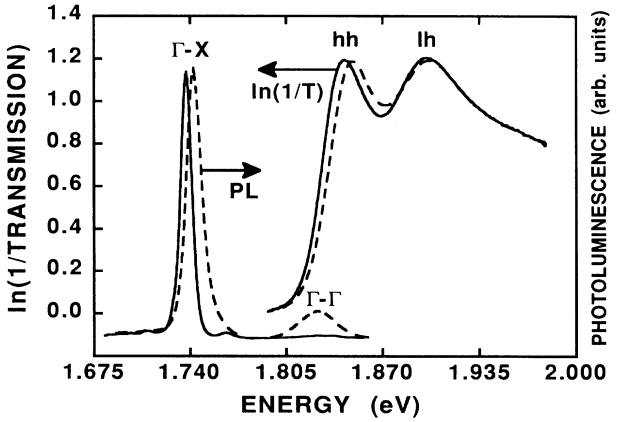

FIG. 2. Blueshifts of the absorption and PL spectra for the (11/30) sample. Solid curves are linear spectra ($I_{\text{linear}}=1$ W/cm^2) and dashed curves are for 10 kW/cm^2 excitation intensity, where $T=15$ K and $E_{\text{excitation}}=1.96$ eV.

energy peak corresponding to indirect-interlayer recombination of X-like electrons in AlAs with Γ-like holes in GaAs (see Fig. 2, solid PL peak labeled Γ-X). In Fig. 2 we also show high-density PL spectra (dashed lines) which we describe in detail in Sec. III. We vary the Γ-X splitting by systematically varying the AlAs layer thickness (11, 18, and 30 monolayers). The linear PL spectra showed that the three Sandia National Laboratory (SNL) samples, GaAs/AlAs (11/30), (11/18), and (11/11), where (m/n) implies m monolayers of GaAs and n monolayers of AlAs, have a Γ-X splitting of 95, 80, and 61 $\pm$ 1 meV, respectively.

III. SPACE-CHARGE EFFECTS

Previously, we reported both experimental and theoretical investigations of the optical-excitation-dependent spatially indirect PL of GaAs/AlAs type-II superlattice.[6] The relevant microscopic mechanisms are exchange and correlation effects in the excited electron and hole plasmas, as well as energy renormalizations due to the optically induced space-charge potential, the latter being the dominant effect. The primary conclusion of this analysis is that a strong potential difference between neighboring layers develops for carrier densities around 10^{12} cm^{-2}. However, the space-charge field has little effect on the valence-conduction-band separation within the same layer since both bands shift essentially parallel.

The low-temperature ($\simeq$15 K) linear absorption spectrum and the excitation-intensity-dependent PL spectra associated with the (11/30) sample are shown in Fig. 2. The linear absorption spectrum shows the heavy-hole (hh) and light-hole (lh) exciton absorption peaks in the vicinity of 1.9 eV. The pump laser at 1.959 eV induces direct Γ-Γ transitions within the GaAs layers. Linear and highly optically excited PL spectra taken at two different excitation intensities are shown.

In order to understand the highly excited PL spectra of type-II structures, we assert that upon optical excitation, which takes place as direct transitions in the GaAs layer, the excited electrons (e) and holes (h) relax on a time scale of a few picoseconds or less[9-11] into quasithermal equilibrium between superlattice layers. The electrons are then distributed according to the law of mass action (Boltzmann factor) between the X bands in the AlAs layers and the Γ point in the GaAs layers. Only the holes occupy the heavy-hole states at the Γ point of the GaAs layer as explained below. The subsequent recombination of the carriers involves, in principle, all of the electron levels as well as the two hole levels. The PL spectra are mainly determined by the relative occupation of the various levels which are governed by carrier lifetimes and the overlap of the electron and hole wave functions.

The high-intensity PL spectrum in Fig. 2 also exhibits an additional peak, labeled Γ-Γ at 1.823 eV, corresponding to the direct recombination in the GaAs layers, as mentioned above. At this density, there is no e-lh photoluminescence, indicating that the chemical potential of the holes is still less than the hh-lh splitting. This transition, however, is evidenced by a shoulder on the high-energy side of the Γ-Γ line at even higher excitation intensities (not shown in Fig. 2). Figure 2 reveals that, with increasing excitation intensity, the Γ-X PL peak shifts up in energy to 1.745 eV ($\simeq$6 meV blueshift).

Spatial separation of the electron and hole plasmas leads to shifts of the valence and conduction bands and hence, of the effective density-dependent energy gap. In this system the space-charge layers cause a band renormalization consisting of two contributions: (1) the exchange-correlation self-energy due to Coulomb-exchange interaction and scattering processes within each plasma and (2) the macroscopic electric field caused by the spatial separation of the charge carriers. Generally, the self-energy leads to a reduction of the energy gap which increases sublinearly with density, as is well known from the theory of a spatially homogeneous, neutral e-h plasma.[16,17] The space-charge potential in the GaAs layer shifts both the conduction and valence bands down by approximately the same amount resulting in negligible shifts of the Γ-Γ transitions and a blueshift of the Γ-X transition. At high densities the energy shift of the Γ-X transition is dominated by the space-charge potential which is roughly proportional to n. In this limit the blueshift arising from the space-charge potential always overcompensates the redshift arising from the self-energy contributions of the single-particle states resulting in a net blueshift of the Γ-X transition.[6]

The experimentally observed increase of the linewidth also contains additional damping effects due to the plasma. These effects lead to an additional linewidth broadening of the PL with respect to the zero-density linewidth allowing for the determination of the quasi-chemical potential.[6] The blueshift of the Γ-X transition is accompanied by a reduction of the splitting $\Delta_{\Gamma\text{-}X}$ which leads to a reduction of the charge separation at very high densities. The electric fields perturb the energies of the system producing a blueshift of the indirect transition resulting in a reduction in the Γ-X energy splitting between conduction-band electron states. A direct analogy can be made with similar electric-field effects in p^+-type δ-doped heterostructures.[18]

IV. NANOSECOND EXPERIMENTS

As shown in Fig. 2, the heavy-hole exciton line in the absorption curve also shifts blue when optically excited. However, as discussed above in Sec. III and quantitatively evaluated in Ref. 14, the space-charge potential shifts the GaAs conduction and valence bands essentially parallel, thus, the blueshift of the hh exciton must be fundamentally different from the blueshift of the Γ-X PL.[6]

In order to study the quasi-cw nonlinearities in the absorption spectra we used nanosecond pump pulses (E_{laser}=2.14 eV, τ_{laser}=7 ns) to excite carriers. We used 100-fs time-correlated broad-band continuum pulses to probe our samples. Nanosecond pulses are well suited for studying type-II systems in the quasisteady state since the real-space charge-transfer rate is subpicosecond[9-11] while the recombination lifetime is many orders of magnitude longer ($\sim\mu s$). Probing the system nanoseconds after excitation allows for the real-space charge transfer to equilibrate with little carrier loss to recombination.

In Fig. 3 we plot pump-intensity-dependent absorption spectra for the SNL (11/30), (11/18), and (11/11) structures at $T=15$ K. The spectra in Fig. 3 show that the inhomogeneously broadened heavy-hole exciton resonance shifts significantly toward higher energies and bleaches with increasing excitation intensity. The amount of broadening needed to reproduce the experimental zero-density spectrum corresponds to well-width fluctuations of approximately one-half monolayer.[19] In contrast, the light-hole exciton shifts very slightly to lower energies and exhibits little reduction in oscillatory strength for the intensities shown. Spectra were taken on different structures in order to investigate the dependence of the observed nonlinearity on the inhomogeneous broadening and the Γ-X splitting. We examine the shift of the hh ex-

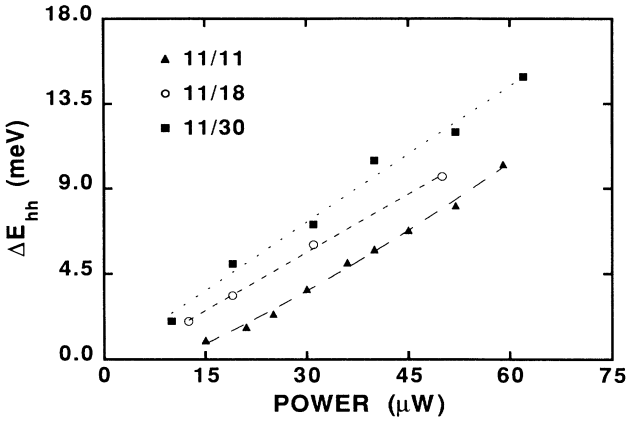

FIG. 4. The blueshift of the heavy-hole exciton vs excitation intensity for the SNL (11/30), (11/18), and (11/11) samples. The lines are drawn to aid the eye.

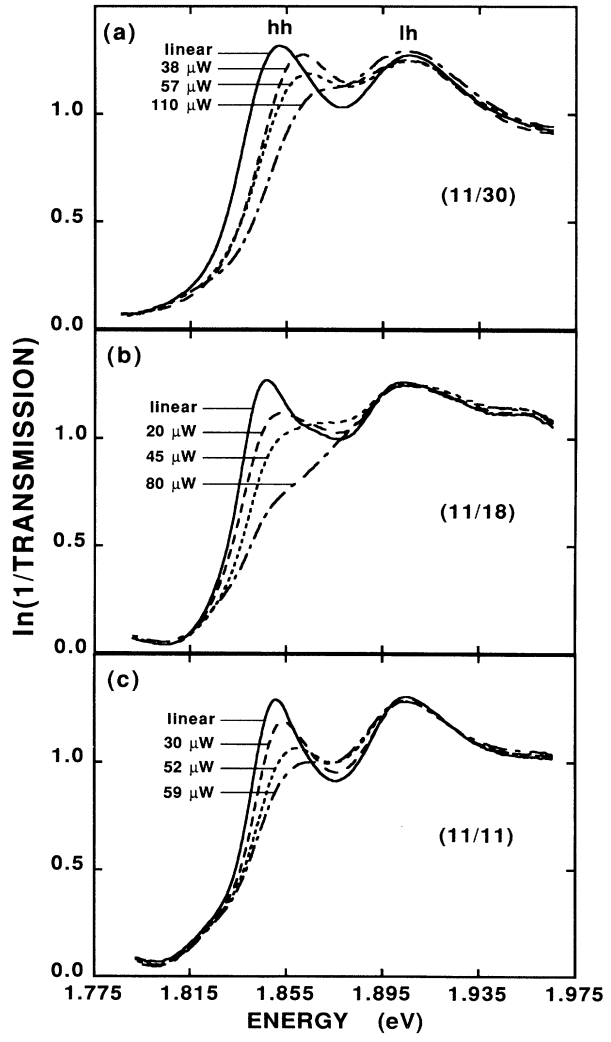

FIG. 3. Excitation-intensity-dependent absorption spectra of structure (a) (11/30), (b) (11/18), and (c) (11/11). $T=15$ K and $E_{laser}=2.14$ eV. The uncertainty in the pump power is less than 40%. The carrier density for the spectrum labeled 45 kW/cm^2 is $\simeq 1.5\times10^{12}$/cm^2.

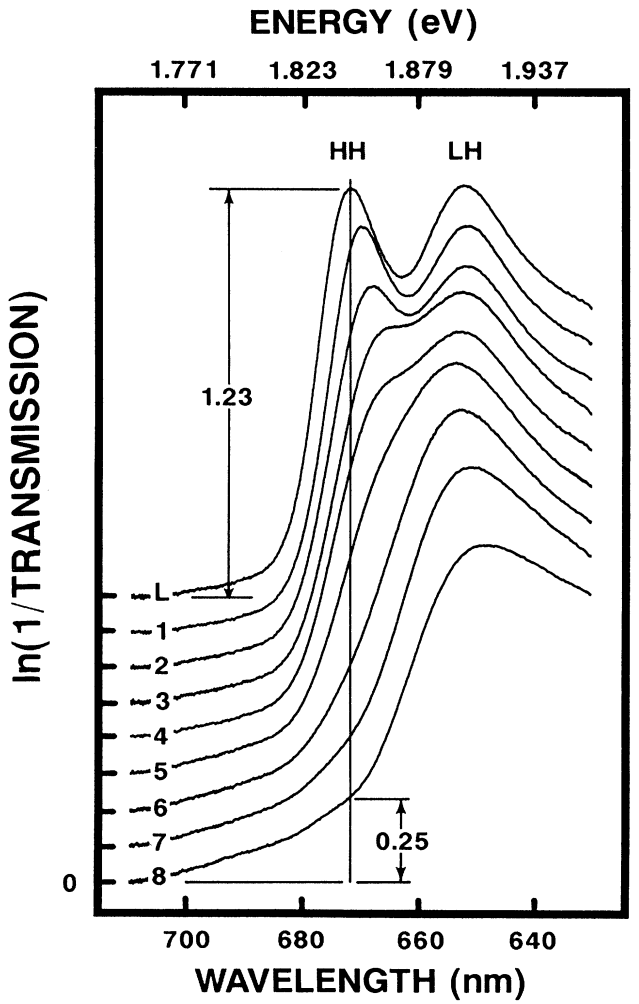

FIG. 5. Excitation-intensity-dependent absorption spectra, $\alpha(I)$. L is the linear spectra ($I_{linear}=1$ W/cm^2), I_{1-8} = 5, 8, 10, 12, 15, 25, 35, 45 kW/cm^2, respectively, $T=15$ K, and $E_{laser}=1.96$ eV.

citon as a function of excitation power for the three SNL samples in Fig. 4, indicating slightly smaller amounts of blueshift in the (11/11) sample which exhibits a narrower hh exciton resonance.

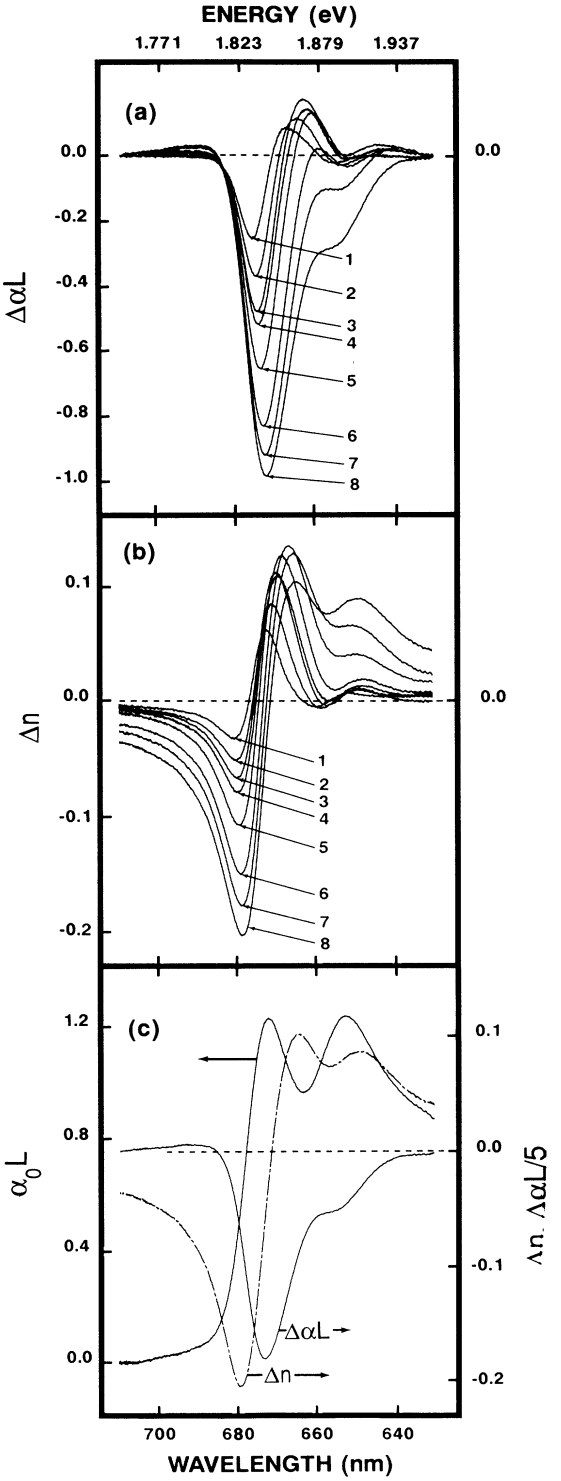

FIG. 6. (a) Absorptive and (b) dispersive changes with respect to the linear spectrum. In (c) we plot the maximum $\Delta\alpha L$ and Δn against the linear spectrum.

In a different experiment we used nanosecond pulses for both pump and probe. We pumped a dye laser ($E_{\text{excitation}}=1.96$ eV) with a copper-vapor laser and used the fluorescence from a DCM dye jet as the broad-band continuum probe. In Fig. 5 we display the development of the absorption spectra with increasing excitation intensity for the SNL (11/30) sample. The antireflection coated sample exhibited maximum absorptive ($\Delta\alpha L$) and dispersive (Δn) changes of 0.98 and -0.2, respectively, for an excitation intensity of 45 kW/cm^2 (see Fig. 6). A $\Delta n=-0.2$ corresponds to a $\pi/2$ phase shift for a 2-μm-thick structure. The changes in the refractive index were obtained using the Kramers-Kronig transformation of the differential absorption. In practice we sum over a finite energy range that is sufficiently large so that the differential absorption vanishes at the end points. In Fig.

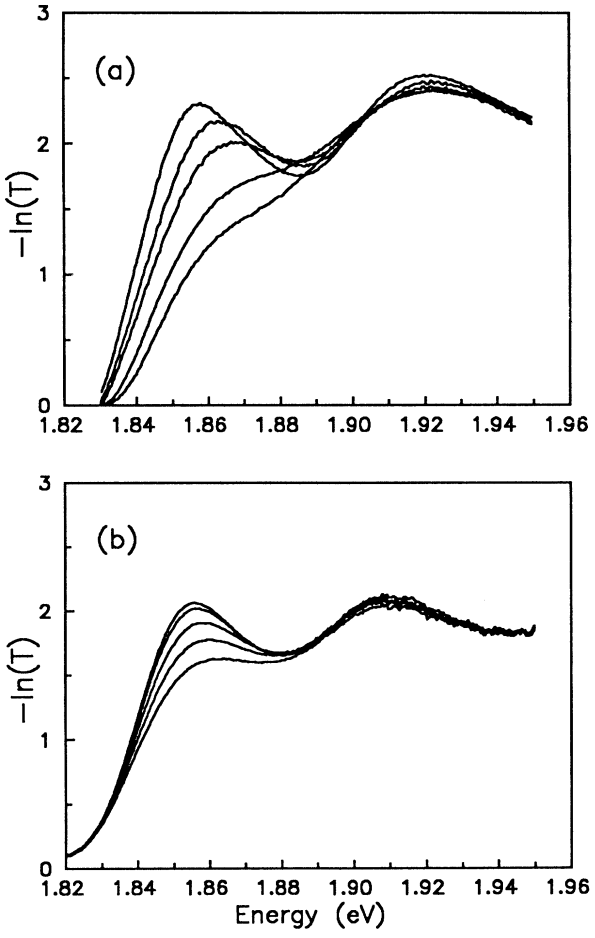

FIG. 7. (a) Nonlinear absorption spectra of the UA sample at 10 K with pump energy of 2.1 eV and the highest pump intensity 20 kW cm^{-2}. The subsequent spectra are taken by stepwise decreasing the pump intensity by factors of 2; the linear spectra is taken for vanishing pump. (b) Same as (a) but at a sample temperature of 77 K and highest pump intensity 7 kW cm^{-2}.

6(c) we superimpose the linear absorption curve with the maximum absorptive and dispersive changes.

Independently we measured the quasi-cw nonlinear absorption spectra of a series of type-II samples grown by molecular beam epitaxy (MBE) at the University of Arizona (UA). Here, we report experimental observations using a sample consisting of 150 periods of 28-Å GaAs wells and 56-Å AlAs barriers with AlGaAs caps on either end, which is similar to the SNL (11/30) sample discussed above. Figure 7(a) shows nanosecond pump-probe spectra obtained for a bath temperature of $T \simeq 10$ K. These results show good agreement with those presented in the top part of Fig. 4, reproducing both bleaching and blueshift of the hh exciton with relatively minor changes around the lh exciton resonance. To study the temperature dependence of the observed optical nonlinearities, and for later comparison with femtosecond pump-probe experiments, we repeated the measurements of Fig. 7(a) with the sample cooled by liquid nitrogen ($\simeq 77$ K). The resulting spectra in Fig. 7(b) show an almost complete disappearance of the hh blueshift. The nonlinear absorption changes consist primarily of exciton bleaching with only a small shift.

V. FEMTOSECOND EXPERIMENTS

We performed two groups of femtosecond (fs) experiments using two sets of different samples. In our first set of fs measurements, performed at SNL, we used 630-nm, 100-fs-duration pump pulses and 100-fs-duration time-correlated white-light continuum probe pulses obtained from a colliding pulse mode-locked ring dye laser amplified in a copper-vapor-laser-pumped dye cell.[20] In Fig. 8 we show the spectrally resolved absorption of the SNL (11/30) structure at various time delays between pump and probe pulses. We observe a small blueshift ($\simeq 4$ meV) of the heavy-hole exciton which develops several hundred femtoseconds after excitation. The blueshift increases (> 15 meV) for the 100-ps spectrum as the quasiequilibrium state is approached. Notice the strong similarity between the 100-ps curve in Fig. 8 and the 100-μW curve in Fig. 3(a). Feldmann *et al.*[9] examined the time dependence of the absorption spectra of type-II GaAs/AlAs superlattices and reported a fast recovery of the absorption in the spectral vicinity of the hh and lh excitons and the split-off band. They attribute this fast recovery to subpicosecond real-space charge transfer. In addition to the excitonic blueshift, saturation, and the absence of gain, we also observe a similar fast recovery of the hh and lh excitons (see Fig. 8; compare curves labeled +500 fs and +1 ps in the vicinity of both the hh and lh excitons).

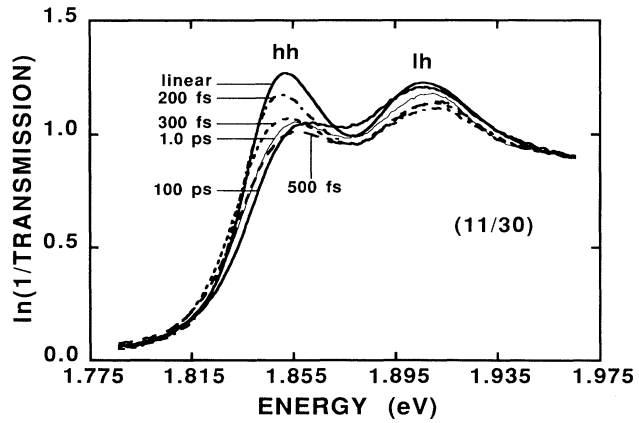

FIG. 8. Femtosecond time-resolved absorption spectra for the (11/30) SNL structure. $P_{exc} = 8.5$ μW (corresponding to a carrier density of $\sim 1 \times 10^{12}/\text{cm}^2$), $E_{exc} = 1.960$ eV, $T = 15$ K.

In our second set of fs experiments, performed at UA, we used fs pumping both resonantly into the inhomogeneously broadened exciton and into the interband absorption region. This pumping was accomplished using a femtosecond laser system with a tunable pump beam. A colliding-pulse mode-locked (CPM) laser utilizing the standard four-prism scheme to correct for intracavity dispersion produces 70-fs pulses at 620 nm. These pulses are then amplified by a six-pass dye amplifier pumped by a copper-vapor laser operating at 8.5 kHz.[20] The amplified pulses have a length of about 80 fs after dispersion correction. We focus these pulses on a jet of ethylene glycol to produce a white-light continuum. Part of this continuum is split off as the broad-band probe. We then use an interference filter to take a 10-nm slice of the remaining continuum as the pump. The pump is amplified by another copper-vapor-laser-pumped, six-pass dye amplifier. After the second amplification, the pulse width is approximately 130 fs. For these experiments, the pump-power density on the samples is about 7×10^8 W cm^{-2}. The signal is approximately linear with pump power. By adjusting the interference filter and/or the dye in the second amplifier, we obtain a completely tunable system. These experiments utilize two different data acquisition systems. The first system uses an optical multichannel analyzer (OMA) which gives spectrally resolved data. The second system is computer controlled and monitors a chosen energy band of the probe signal as a function of the time delay between the pump and probe pulses. The probe beam and a reference beam are sent into a spectrometer and are detected by photomultiplier tubes (PMT's). The signals are digitized by a fast analog-to-digital converter (ADC) with 10-bit accuracy and sent to the computer via a Camac system. The pump pulse for each set of probe pulses is also digitized and sent to the computer.

With this system we first repeat the experiment with pumping into the interband absorption region (at 636 nm in this case) using the UA type-II sample. Figure 9 shows the results indicating bleaching and a blueshift of the hh and lh exciton peaks, in good agreement with Fig. 8. Figure 10 shows the spectrally resolved data for the same sample, but for pumping at 668 nm, i.e., directly into the hh exciton peak. Again, we see pronounced exciton bleaching and a blueshift of the hh and lh exciton peaks. By $\simeq 3$ ps the lh peak has no blueshift, the bleaching begins to recover, and is completed by 100 ps. By $\simeq 3$ ps also the hh peak has begun to recover from the bleach-

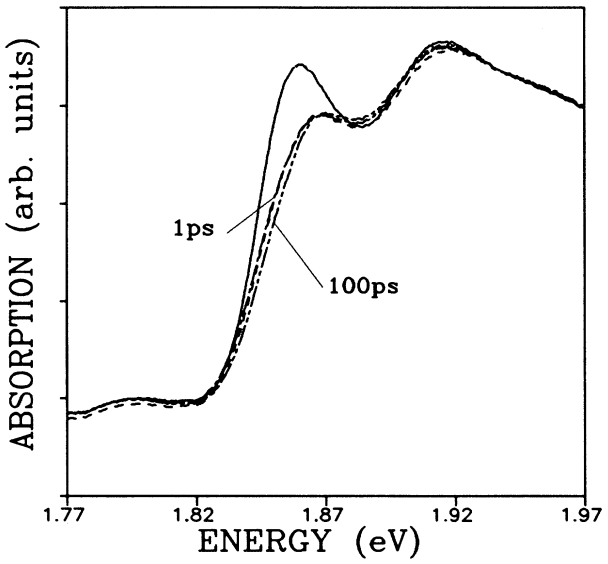

FIG. 9. Time-resolved absorption spectra for the UA sample. The pump is centered at 1.949 eV.

ing. Between 3 and 100 ps, the low-energy side of the heavy hole *rebleaches*. We also see large induced absorption between the heavy-hole and light-hole peaks which is much smaller in the interband pumping case. These results are qualitatively similar, but greater in magnitude than those for pumping into the interband absorption region.

While resonantly pumping the hh exciton peaks, the time-resolved data-acquisition system was used to probe on and around both the hh and lh peaks. In Fig. 11(a) we present the bleaching dynamics for several fixed pump-and-probe wavelengths [pump at hh and probe at hh (solid line); pump at hh and probe at lh (dashed line); pump at lh and probe at lh (dashed-dotted line)] on a timescale of 10 ps, and in Fig. 11(b) we extend the time scale to cover 500 ps. Figure 11 shows a large initial bleaching with a recovery of the absorption within a few picoseconds. This fast recovery is particularly strong at the lh exciton if the pump is centered at that resonance.

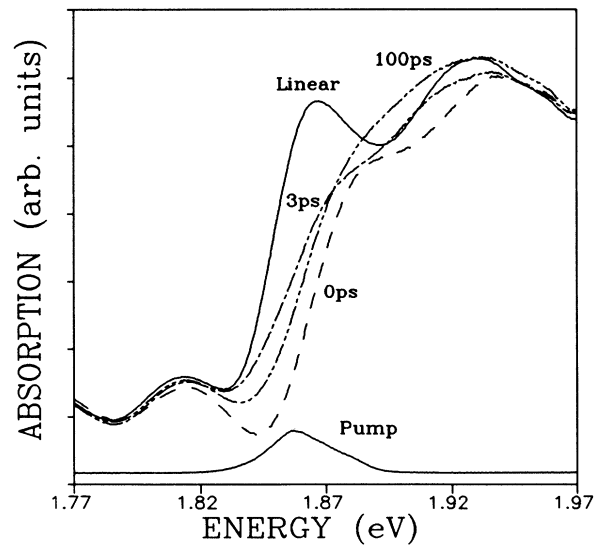

FIG. 10. Same as Fig. 9 but pumping at 1.856 eV, i.e., directly into the heavy-hole exciton peak.

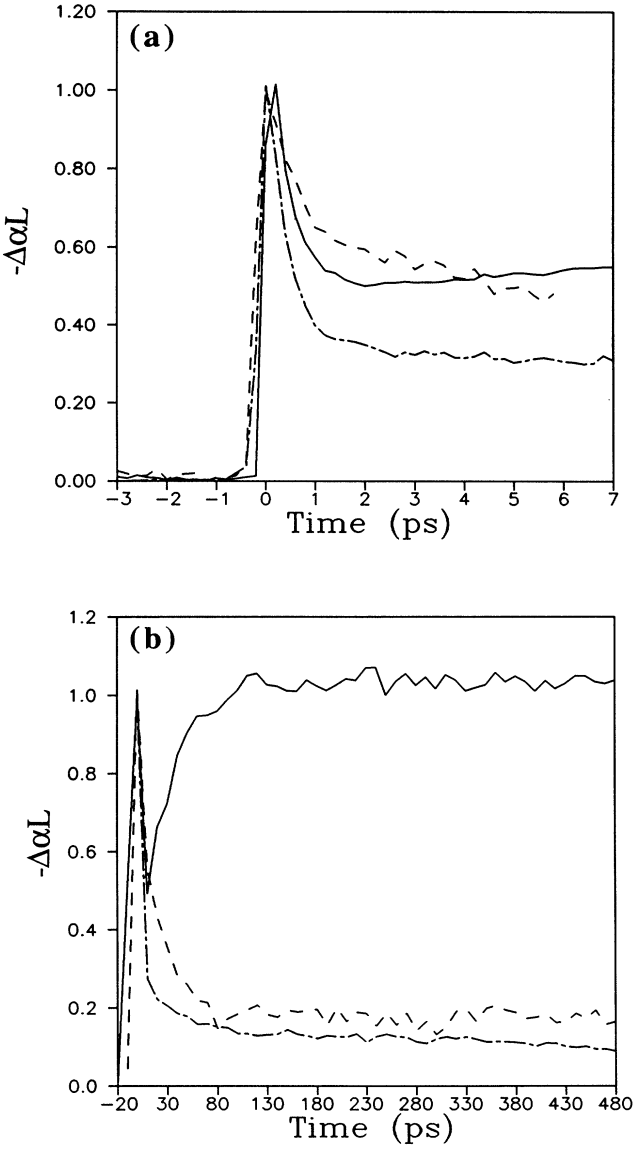

FIG. 11. Time dependence of the bleaching of Figs. 9 and 10 for fixed frequencies, (a) with femtosecond resolution, and (b) on a 100-ps time scale. For excitation at the hh resonance we show curves for probing at the hh (solid line) and lh (dashed line) exciton resonances. The dashed-dotted line represents the temporal behavior for pumping and probing at the lh resonance.

On the other hand, the hh exciton bleaching does not recover on a 500-ps time scale. When the hh exciton is pumped, the lh bleaching shows essentially only the ultrafast recovery and nothing else. The hh, however, shows again a *rebleaching* on the 100-ps time scale. One should note that the levels in the long time curves do not always match the levels in the short time graphs. This occurs because the time resolution of the longer curves is less than that of the short time curves. Thus, the system is likely to miss the extrema, e.g., the minimum of the initial recovery. Note also that the absolute values of the bleaching shown in Fig. 11 depend on the absorption at the pump wavelength. Therefore the case of pumping into the hh and pumping into the lh should not be compared quantitatively.

VI. THEORETICAL ANALYSIS

In this section we sketch our theoretical analysis of the experimental results. We concentrate on the absorption in the GaAs layer, i.e., the Γ-Γ transition. For the nanosecond pump-probe experiments one can assume complete *e-h* charge separation with the electrons in the AlAs layer and the holes in the GaAs barriers. Hence, the nonlinear spectra of the GaAs can be described assuming that a certain density of holes is present without any electrons. The holes are distributed within the various in-plane bands according to Fermi functions, the subbands being in general all the subbands of both the hh and the lh states. Such a plasma in a semiconductor layer causes many-body modifications of the optical properties of that layer, which are in principle quite similar to the plasma effects of a homogeneous *e-h* plasma in a type-I or bulk system. Apart from these local effects, which we will discuss below, there are the effects caused by the electric field which is induced by the charge separation of electrons and holes. A first quantitative analysis of these global field effects on the photoluminescence transitions of type-II systems has been discussed in Ref. 6. A detailed theoretical analysis of these effects is given in Ref. 14, where a model calculation is presented for the absorption of a GaAs layer where no electrons are present and only the hh states are occupied, which is appropriate if the chemical potential of the heavy holes is less than the hh-lh splitting. The calculations were done for the lowest subband only, which is justified in very thin GaAs layers, where the subband separations are large. In Ref. 14 we also solve the coupled Schrödinger and Poisson equations for the carriers to show quantitatively that the influence of the space-charge field on the absorption transition is of minor importance as long as the Γ-X splitting is large compared to the chemical potential of the electrons in the X valley.

In Ref. 14 some homogeneously broadened spectra were computed to illustrate the various many-body effects. However, as mentioned in the previous sections of the present paper, in order to compare with experimental data, one has to account for the well-width fluctuations which lead to pronounced inhomogeneous broadening of the spectra. The main effect here is simply a shift of the in-plane band, since fluctuations $\Delta L = L - L_0$ around the average well widths L_0 yield changes $\Delta E(L)$ of the confinement energies. If the scale of the interface roughness is on the order of the exciton Bohr radius, one can assume that the averaging of well thicknesses follows effectively a continuous distribution although the actual thickness variations are always multiple integers of the lattice constant. In the case of multiple quantum wells, inhomogeneities occur both within each layer, i.e., as a function of the x,y coordinates for fixed z, and in growth direction, since the different quantum wells may have different thicknesses. In order to account for this effect we take the homogeneously broadened spectra $\alpha_{\text{hom}}(\hbar\omega)$ and subject them to the superposition

$$\alpha_{\text{inhom}}(\hbar\omega) \propto \int dL\, e^{-(L-L_0)^2/\sigma^2} \alpha_{\text{hom}}(\hbar\omega + \Delta E(L)) \,. \quad (3)$$

A further effect of the inhomogeneity arises when the structure is optically excited. As a consequence of the in-plane inhomogeneities one can expect that the plasma will try to localize in the regions of wider wells in order to reduce its confinement energy. With regard to the bleaching of excitons this will favor the bleaching of the energetically lowest-lying excitons, i.e., the low-energy part of an inhomogeneously broadened exciton peak. The complete modeling of these effects poses a vast numerical problem, since the calculation of one spectrum requires knowledge of all homogeneous spectra for all densities. Furthermore, it also leads to a self-consistency problem, since fluctuations in the carrier energies lead to fluctuations in the local-carrier densities which in turn lead to fluctuations in the many-body effects. The investigation of this complex, spatially inhomogeneous arrangement exceeds by far our current numerical capabilities. Therefore, we model the system as inhomogeneously broadened using Eq. (3) to compute the full spectra from the homogeneous ones.

Generally, in bulk or most type-I structures (for deviations see Ref. 21) increasing excitation first bleaching of the exciton without any significant shift until, at high densities, a gain region forms.[21–25] The point where the absorption curve crosses zero, i.e., the sum of the chemical potentials of the electron and hole plasmas, shifts to higher energies with increasing density since the bandgap shrinkage due to the plasma is always less than the increase of the chemical potential. The absorption spectrum around the chemical potential experiences significant Coulomb enhancement which may lead to an absorption peak, the so-called Mahan exciton. This absorption peak is observed at high-excitation intensities, even though no bound electron-hole-pair state exists.

In type-I structures the simultaneous occurrence of optical gain clearly distinguishes the Coulomb-enhancement peak from the low-density exciton resonance.[14] Carrier inversion is inhibited in a pure type-II system because the electrons are separated from the holes. Consequently, the gain region of a type-I absorption spectrum is replaced by a zero-absorption region in type-II structures. The hole chemical potential coincides with the onset of absorption

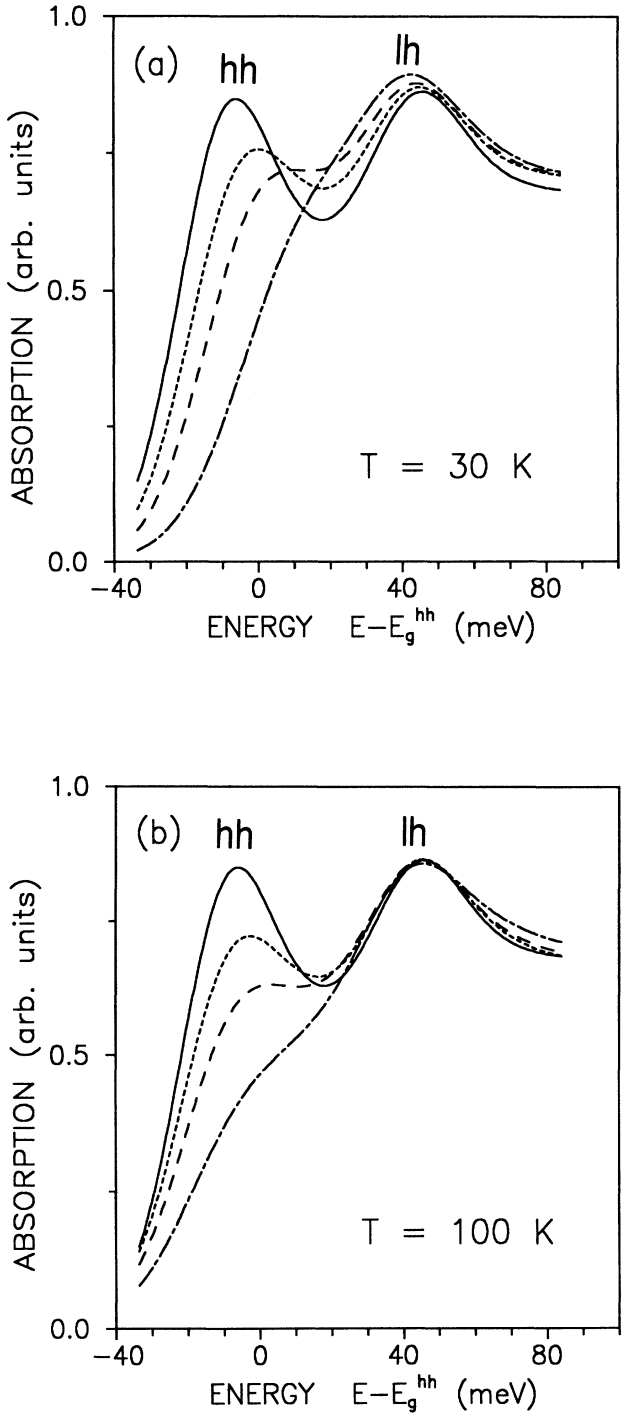

FIG. 12. Computed absorption spectra for type-II quantum wells with GaAs well thickness of 30 Å. The spectra are for the plasma densities $na_0^2=0.2$ (short-dashed line), 0.4 (medium-dashed line), and 0.8 (long-short-dashed line). The linear spectra are shown as solid lines and a_0 is the bulk-exciton Bohr radius. (a) Plasma temperature is 30 K; (b) plasma temperature $T=100$ K. The underlying homogeneous linewidth is 5 meV [full width at half maximum (FWHM)] and the additional inhomogeneous linewidth [see Eq. (3)] is 28 meV (FWHM).

for the type-II system. The blueshift of the hh observed in the nanosecond experiments at low temperatures and elevated densities is then simply the so-called Burstein shift known from type-I systems with the difference that only the hole quasi-Fermi level contributes in the type-II case. Due to the absence of a spectral region with optical gain in a highly excited low-temperature type-II system, where electron transfer to the AlAs layers has occurred, the Coulomb-enhancement resonance above the quasi-chemical potential appears as a blueshifted exciton. Such Coulomb enhancement peaks in semiconductors have been discussed for the case of n-doped type-I systems.

It is worthwhile to note that a blueshift of the exciton absorption in narrow type-I quantum wells was observed and attributed to exciton-exciton interaction.[21] As we have shown in Ref. 14, the blueshift of the heavy-hole exciton in our type-II structures is consistently explained by the many-body effects associated with the presence of a hh plasma in the GaAs layer without including exciton-exciton effects. We computed these shifts by solving the generalized Wannier equation assuming complete separation of electron and hole plasmas. As examples of our theoretical results we present in Fig. 12 computed density-dependent absorption spectra for two different plasma temperatures. Figure 12(a) shows spectra at low plasma temperature ($T=30$ K) exhibiting good qualitative agreements with those of Figs. 3(a) and 7(a). The analysis shows that the observed hh exciton blueshift is in fact the Burstein shift of the Mahan exciton at the Fermi edge. For all densities shown, the reduced hh band gap is below the zero-density hh exciton resonance.

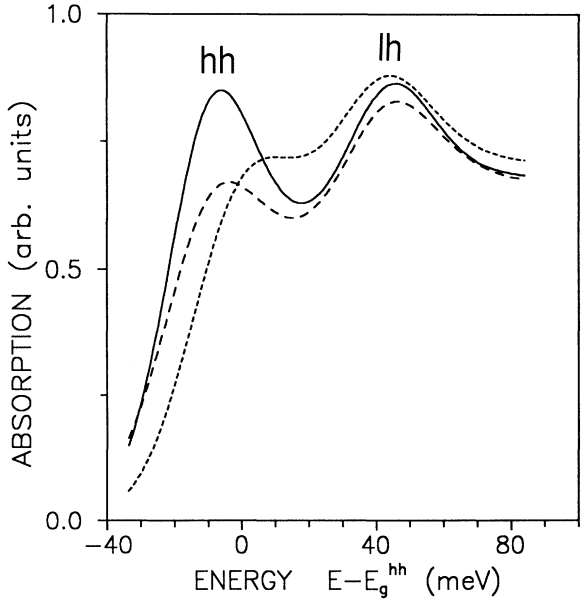

FIG. 13. Computed type-II absorption spectra for a hole plasma $na_0^2=0.4$ and the plasma temperatures 30 K (short-dashed line) and 300 K (long-dashed line). The linear spectrum (solid line) and all other parameters are the same as in Fig. 12.

For the lh exciton we find a small redshift with relatively little loss in oscillator strength. This shift is caused by the screening due to the hh plasma (generalized Coulomb hole). The results in Fig. 12(b) compare well with the nanosecond spectra shown in Fig. 7(b) showing the absence of the hh exciton blueshift for elevated hh plasma temperatures. The elevated plasma temperature leads to reduced hole phase-space filling which in turn causes the vanishing of the hh shift.[14]

To analyze the delayed onset and full development of the magnitude of the blueshift in the femtosecond measurements of Figs. 8–10 we show in Fig. 13 computed inhomogeneously broadened spectra for a fixed-hole plasma density at 30 and 300 K. Although we assume a quasithermal equilibrium, the 300-K calculation can serve as a model of the situation in the femtosecond experiment for the case of interband excitation, where we have initially a very hot carrier distribution. Indeed we find a striking similarity between the 300-K curve of Fig. 13 with the 300-fs spectrum in Fig. 8. This similarity comprises not only the bleaching and shift of the hh exciton, but also applies to the lh exciton, which at early time as well as high temperatures is bleached considerably. Note that in our calculation no occupation of the lh is assumed, so that the bleaching is a consequence of the screening of the *e-h* Coulomb interaction only. Comparing the 30-K curve of Fig. 13 with the 100-ps spectrum in Fig. 8 again supports our interpretation of the experimental spectra in terms of carrier cooling.

Concerning the different shifts of the nanosecond spectra for different samples we studied the influence of different inhomogeneous broadening. Taking the same homogeneously broadened spectra which were inhomogeneously broadened to obtain Fig. 12(a), we show in Fig. 14 also inhomogenously broadened spectra, but now with only half the amount of inhomogeneous broadening. The comparison of Figs. 12(a) and 14 reveals that the amount of observable hh exciton blueshift slightly decreases with decreasing inhomogeneous broadening, solely as a consequence of the different superpositions of the homogeneous spectra. Qualitatively the same can be seen by comparing the spectra of Fig. 3(a) with those of Fig. 3(c). Also, in the case of reduced inhomogeneous broadening we find a slight bleaching of the lh exciton as well as a somewhat stronger redshift. This is to be expected, since the homogeneous lh spectra always exhibit a slight bleaching and redshift.[14]

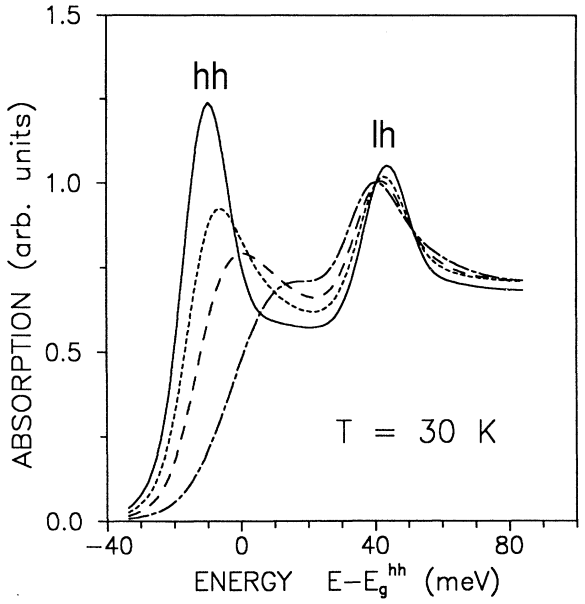

FIG. 14. Same as Fig. 12(a) but with half the inhomogeneous broadening.

VII. SUMMARY AND DISCUSSION

In summary, the observed nonlinearities are caused by the excited hole and electron plasmas which separate on a subpicosecond time scale with respect to both spatial and momentum coordinates. In our low-temperature nanosecond spectra we observe bleaching and blueshift of the heavy-hole exciton and only very small changes (slight redshift and minute saturation) at the lh exciton. We explain the hh blueshift as the Burstein shift for a type-II system and identify the high-density absorption peak as Coulomb enhancement peak or Mahan exciton. A higher hh plasma temperature leads to a strong reduction of the effects of Pauli blocking which are responsible for the Burstein shift. The high-temperature spectra yield exciton saturation without appreciable shift.

We explain the delayed onset and full development of the magnitude of the blueshift in the femtosecond measurements through thermalization of the electrons and holes. Initially electrons and holes are injected into the conduction and valence bands with excess energy depending on the pump wavelength. After the initial rapid cooling by LO-phonon emission, complete thermalization to the lattice temperature occurs on the time scale of hundreds of picoseconds via acoustic-phonon emission. For the hot plasma there is little blueshift of the exciton resonance. The cooling of the plasmas occurs on a $\sim$100-ps timescale because at low temperatures acoustic phonons do not play a significant role in scattering processes. This is consistent with our observation and calculation of the disappearance of the hh exciton blueshift in the nanosecond experiments with increasing temperature (Fig. 7).

The spectrally resolved data in Fig. 11 display quite similar behavior. The bleaching levels and blueshifts are somewhat larger for the resonant pump because cool carriers are excited directly at the inhomogeneously broadened hh exciton peak. The hh and lh excitons share the same electron level. Therefore, as long as excited electrons are present in the GaAs layer, they block both the hh and lh transitions. As the electrons scatter from the Γ point in the GaAs to the X point in the AlAs, the heavy-hole peak partially recovers from the bleaching[9] and blueshift in less than 3 ps. However, the bleaching of the low-energy states continues between 3 and 100 ps due to cooling of the holes. The holes created with excess en-

ergy slowly relax to the bottom of the band and block the lower-energy portions of the transition. The holes remain in this band for a long period of time because the recombination with the electrons is indirect in both real and reciprocal space. The behavior of the lh resonance supports the analysis in terms of hole cooling. The lh peak initially bleaches and blueshifts due to blocking of its electron state. However, as the electrons rapidly scatter to the AlAs barrier, the lh peak loses its blueshift and a good portion of its bleaching. The remaining bleaching is due to Coulomb screening of the transition by the heavy holes.

ACKNOWLEDGMENTS

The Sandia National Laboratories (SNL) group thanks A. Owyoung for technical discussions. W.S.F. thanks Professor J. S. Harris, Standord University, for support. SNL research is supported by U.S. Department of Energy Contract No. DE-AC04-76DP00789. The Arizona group is supported by grants from NSF, ARO, Air Force Office of Scientific Research, SNL, Optical Circuitry Cooperative, and the Pittsburgh Supercomputer Center. R.B. acknowledges financial support through the Deutsche Forschungsgemeinschaft (Federal Republic of Germany).

---

*Also at Solid State Electronics Laboratory, Stanford University, Stanford, CA 94305.

†Permanent address: Philips Research Lab., Redhill, Great Britain.

‡Also at Physics Department, University of Arizona, Tucson, AZ 85721.

[1]J. Ihm, Appl. Phys. Lett. **50**, 1068 (1987).

[2]G. Danan, B. Etienne, F. Mollot, and R. Planel, Phys. Rev. B **35**, 535 (1987).

[3]E. Finkman, M. D. Sturge, M. H. Meynadier, R. E. Nahory, M. C. Tamargo, D. M. Hwang, and C. C. Chang, J. Lumin. **39**, 57 (1987).

[4]K. J. Moore, P. Dawson, and C. T. Foxon, J. Phys. (Paris) Colloq. **48**, C5-525 (1987).

[5]B. A. Wilson, C. E. Bonner, R. C. Spitzer, P. Dawson, K. J. Moore, and C. T. Foxon, J. Vac. Sci. Technol. **4**, 1156 (1988).

[6]G. R. Olbright, J. Klem, A. Owyoung, T. M. Brennan, R. Binder, and S. W. Koch, J. Opt. Soc. Am. B **7**, 1473 (1990).

[7]G. Danan, F. R. Ladan, F. Mollot, and R. Planel, Appl. Phys. Lett. **51**, 1605 (1987).

[8]M.-H. Meynadier, R. E. Nahory, J. M. Worlock, M. C. Tamargo, J. L. de Miguel, and M. D. Sturge, Phys. Rev. Lett. **60**, 1338 (1988).

[9]J. Feldmann, R. Sattmann, E. O. Göbel, J. Kuhl, J. Hebling, K. Ploog, R. Muralidharan, P. Dawson and C. T. Foxon, Phys. Rev. Lett. **62**, 1892 (1989).

[10]P. Saeta, J. F. Federici, R. J. Fischer, B. I. Greene, L. Pfeiffer, R. C. Spitzer, and B. A. Wilson, Appl. Phys. Lett. **54**, 1681 (1989).

[11]G. R. Olbright, W. S. in Fu, J. Klem, T. E. Zipperian, R. Binder, and S. W. Koch, in *Ultrafast Phenomena VII,* edited by C. Harris, E. Ippen, and A. H. Zewail (Springer-Verlag, Berlin, 1990).

[12]G. R. Olbright, J. Klem, W. S. Fu, G. R. Hadley, and S. W. Koch, *Large Optical Nonlinearities Arising from Space-Charge Layers in GaAs/AlAs Staggered Alignment Superlattices, Optical Society of America Annual Meeting, 1989,* Technical Digest Series (Opt. Soc. of America, Washington, D.C., 1989), p. 16.

[13]G. R. Olbright, W. S. Fu, A. Owyoung, J. F. Klem, R. Binder, I. Galbraith, and S.W. Koch, Phys. Rev. Lett **66**, 1358 (1991).

[14]R. Binder, I. Galbraith, and S. W. Koch Phys. Rev. B **44**, 3031 (1991).

[15]See the following and references therein: H. W. van Kesteren, E. C. Cosman, P. Dawson, K. J. Moore, and C. T. Foxon, Phys. Rev. B **39**, 13 426 (1989); P. Dawson, C. T. Foxon, and H. W. van Kesteren, Semicond. Sci. Technol. **5**, 54 (1990).

[16]See, e.g., H. Haug and S. Schmitt-Rink, Prog. Quantum Electron. **9**, 3 (1984); R. Zimmermann, *Many-Particle Theory of Highly Excited Semiconductors* (Teubner, Leipzig, 1987); S. Schmitt-Rink, D. S. Chemla, and D. A. B. Miller, Adv. Phys. **38**, 89 (1989).

[17]H. Haug and S. W. Koch, *Quantum Theory of the Optical and Electronic Properties of Semiconductors* (World Scientific, Singapore, 1990).

[18]P. Ruden and G. H. Döhler, Phys. Rev. B **27**, 3538 (1983).

[19]W. S. Fu, G. R. Olbright, A. Owyoung, J. Klem, R. Biefeld, and G. R. Hadley, Appl. Phys. Lett. **57**, 1401 (1990).

[20]W. H. Knox, M. C. Downer, R. L. Fork, and C. V. Shank, Opt. Lett. **9**, 552 (1984).

[21]N. Peyghambarian, H. M. Gibbs, J. L. Jewell, A. Antonetti, A. Migus, D. Hulin, and A. Mysyrowicz, Phys. Rev. Lett. **53**, 2433 (1984).

[22]R. Binder, S. W. Koch, I. Galbraith, W. S. Fu, A. Owyoung, G. R. Olbright, R. Pon, G. Khitrova, and H. M. Gibbs, *Optical Nonlinearities in Type-II and Type-I Semiconductor Quantum Wells, Conference on Lasers and Electro-Optics, 1991* (Opt. Soc. of America, Washington, D.C.), pp. 114 and 115.

[23]See the following and references therein: Y. H. Lee, A. Chavez-Pirson, S. W. Koch, H. M. Gibbs, S. H. Park, J. Morhange, A. Jeffery, N. Peyghambarian, L. Banyai, A. C. Gossard, and W. Wiegmann, Phys. Rev. Lett. **57**, 2446 (1986); W. Z. Lin, L. G. Fujimoto, E. P. Ippen, and R. A. Logan, Appl. Phys. Lett. **50**, 124 (1987).

[24]W. S. Fu, G. E. Poirier, R. P. Bryan, J. F. Klem, G. R. Olbright, A. Paul, R. Binder, S. W. Koch, and J. S. Harris, *Femtosecond Gain Dynamics in Semiconductors, Quantum Optoelectronics, 1991,* Technical Digest Series (Opt. Soc. of America, Washington, D.C., 1991), Vol. 7, pp. 144–147.

[25]B. Fluegel, K. Meissner, R. Pon, G. Khitrova, H. M. Gibbs, and N. Peyghambarian, *Femtosecond Measurements of Hole Relaxation in a GaAs-AlAs Type-II Structure, Quantum Electronics Laser Science, 1991,* Technical Digest Series (Opt. Soc. of America, Washington, D.C., 1991), pp. 250–252.